**RESEARCH ARTICLE**

# Satellite imagery and modeling contribute understanding cover crop effect on nitrogen dynamics and water availability

Giorgia Raimondi[1] · Carmelo Maucieri[1] · Maurizio Borin[1] · José Luis Pancorbo[2] · Miguel Cabrera[3] · Miguel Quemada[2]

**Abstract**

Cover crops (CCs) can affect the cropping systems' N dynamics and soil water content (SWC), but optimizing their potential effects requires knowledge of their growth pattern, N accumulation, and mineralization. For this purpose, a 3-year field experiment was initiated in northeast Italy involving a maize-soybean rotation. The objectives of this study were to (i) evaluate the use of time series vegetation indices (VIs) obtained from the Sentinel-2 satellite for monitoring the growth of CCs and estimating their biomass and N uptake at termination; (ii) investigate the effects of different CCs on cash crop yield and SWC; and (iii) use the simulation model CC-NCALC to predict the nitrogen contribution of CCs to subsequent cash crops. Three CC systems were tested: a fixed treatment with triticale; a 3-year succession of rye, crimson clover, and mustard; and a control with no CCs. Satellite imagery revealed that rye and triticale grew faster during the winter season than clover but slower compared to mustard, which suffered a frost winterkilling. Both grasses and mustard produced greater biomass at termination compared to clover, but none of the CC species affected SWC or yield and N uptake of the cash crop. A net N mineralization of all the CC residues was estimated by the model (except for the N immobilization after triticale roots residues). During the subsequent cash crop season, the estimated clover and mustard N released was around 33%, and the triticale around 3% of their total N uptake, with a release peak 2 months after their termination. The use of remote sensing imagery and a prediction model of CC residue decomposition showed potential to be used as instruments for optimizing the CCs utilization and enhancing cropping water and N fertilization management efficiency; however, it must be further analyzed with other CCs species, environmental conditions, and cropping systems.

**Keywords** Residue's N release · Soil water content · Mineralization · Remote sensing

## 1 Introduction

Planting cover crops (CCs) is an acknowledged practice to promote agricultural sustainability by provisioning several agroecosystem services (Wallander et al. 2021) which, among other things, can enhance the cropping systems' fertilization (Dabney et al. 2001; Gabriel et al. 2016) and

irrigation management efficiency (Nowak et al. 2022). Nevertheless, enhancing the role of CCs as a suitable solution to reduce chemical fertilizer and water inputs requires a deep knowledge of their growth, nutrient accumulation, and further mineralization (Robertson et al. 2014). Within this frame, the use of satellite images and modeling to monitor the CCs growth and predict their nitrogen (N) contribution to cash crops can be of crucial importance to support farmers and technical advisors to better manage water and N inputs reducing potential environmental impacts and increasing the sustainability of their agricultural systems.

Cover crops performance varies depending on several factors such as planting date and termination, CC species, agricultural management, soil type, elevation, and local and annual climate variability (Poeplau and Don 2015; Lee et al. 2016; Hively et al. 2020). All these factors can affect the CCs' total biomass accumulation, soil coverage, and nutrient uptake, which are directly related to the

✉ Giorgia Raimondi
giorgia.raimondi@unipd.it

[1] Department of Agronomy, Food, Natural resources, Animals and Environment–DAFNAE, University of Padua, Viale dell'Università 16, 35020 Legnaro, PD, Italy

[2] Department of Agricultural Production, Universidad Politécnica de Madrid, CEIGRAM, Senda del Rey 18, 28040 Madrid, Spain

[3] Department of Crop and Soil Sciences, University of Georgia, Athens, GA 30602, USA

INRAE ⧉ Springer

magnitude of agroecosystem services the CCs can provide (Jennewein et al. 2022) both during their growing season and after their termination. For instance, a high winter biomass accumulation is usually related to a high nutrient uptake, which can reduce the soil nutrient concentration potentially leachable (Prabhakara et al. 2015). In addition, the quantity of residues after the CC termination can contribute to the N nutrition of the subsequent crops (Thapa et al. 2018) and affect the soil water content (SWC) available to them (Blanco-Canqui et al. 2020). After termination, CC residues (both incorporated or surface-applied) can release N that might contribute to the cash crop nutrition (Quemada et al. 1997; Cabrera et al. 2005; Thapa et al. 2018, 2022). In addition, their presence during winter can improve soil physical properties (reducing soil bulk density, increasing soil aggregates and water stability, and improving water infiltration and saturated hydraulic conductivity) (Bruce et al. 1991) and increase SWC (Malone et al. 2007). However, on the opposite side, the CC presence can potentially result in nutrients (N) and water competition with the following cash crop, risking impairing the final yield production and quality (Alonso-Ayuso et al. 2014; Gabriel et al. 2014, 2019; Alvarez et al. 2017).

The extent of the N release from the CC residues is strongly affected by multiple factors (residues' quality, management, and environmental conditions) (Poffenbarger et al. 2015; Wagger et al. 1998), and it might even result in N immobilization (Rosolem et al. 2018), in the short period, rather than in an additional N contribution. Indeed, it is still unclear if and to what extent CCs can contribute to the cash crop's N requirements and help reduce the reliance on N fertilizers (Wittwer and van der Heijden 2020). This might vary a lot among CC species, but even in the case of legume CCs (reported to fix more than 100 kg N ha$^{-1}$ year$^{-1}$), it is difficult to predict the actual N quantity available for the subsequent cash crop (Thorup-Kristensen et al., 2003; Büchi et al. 2015).

In this context, it is important to take into consideration that CCs are usually adopted by farmers whose priority is economic success, and they often find the disadvantages of this practice more evident than the advantages (Bergtold et al. 2019). Therefore, the development of reliable tools to monitor the CCs' growth and estimate their possible contribution or immobilization of the N resources might be of utmost importance to evaluate both the advantages and disadvantages related to their adoption in specific sites. This might help the farmers to manage the CC introduction in their agricultural systems maximizing the potential benefit and reducing the potential adverse effects. This is getting even more important after recent global events (including the global pandemic and Ukraine's invasion by Russia) that led to unprecedented N fertilizer price increases threatening the global food and energy supply.

The use of remote sensing techniques to detect and spatialize CCs' growth dynamics and ground cover might be an important tool to investigate the performance of CCs, especially on a large scale, helping the farmers to better manage the CCs according to site-specific needs (Thieme et al. 2020). The retrieval of vegetation indices (VIs), such as the Normalized Difference Vegetation Index (NDVI), from remote sensing imagery is a widespread technique to investigate CCs growth status (Kariyeva and Van Leeuwen 2011; Fan et al. 2020; Gabbrielli et al. 2022). The importance of these remote assessments is gaining increased attention, and it has also been promoted as a first step to defining effective policies that promote the adoption of CCs (Hively et al., 2015; Fan et al. 2020; Nowak et al., 2020). In addition to NDVI, a variety of reflectance-based VIs have been proposed to assess different agronomic variables depending on the regions of the electromagnetic spectrum used. Many of the VIs are based on bands in the visible and near-infrared (NIR) due to the spectral differences between soil and green biomass in these regions caused by the strong chlorophyll absorbance in the visible and the high reflectance of healthy vegetation in the NIR (Daughtry et al. 2000). The VIs based on the red edge region (680–780 nm) enhance the sensitivity to chlorophyll content, and because of the link between chlorophyll and leaf N content, they have the potential to estimate CC N uptake (Yoder and Pettigrew-Crosby 1995; Chen et al. 2010). Also, satellite imagery offers multiple benefits (the capability of acquiring time series images with short revisit time, the wide extension covered by a single image, and the availability of open-access products) that make it suitable for monitoring the performance of CCs in real field conditions (Sishodia et al. 2020).

While the use of remote sensing techniques can be a valid instrument for the CCs' growth monitoring, specific models are required to investigate the CCs' N contribution to the subsequent crop. For this purpose, a web-based model named CC N calculator (CC-NCALC) (developed by the University of Georgia; Woodruff et al. 2018) was created to predict N mineralized or immobilized from decomposing CC residues. The model's main purpose is to help farmers manage N more efficiently, preventing potential problems related to over or under-fertilization. The model, which takes into account many factors affecting the N release from CCs residues (Woodruff et al. 2018; Thapa et al. 2022), has been proposed as a decision support tool to adjust the N fertilizer dose for the cash crops cultivated after CCs seasons.

The present study, conducted in a 3-year maize-soybean rotation in northeast Italy, is aimed at (i) evaluating the efficacy of utilizing time series VIs obtained from the Sentinel-2 satellite for monitoring the growth of CCs, estimating their biomass and N uptake at the termination date; (ii) investigating the various effects of different CCs on cash crop yield and SWC; and (iii) using the simulation model

"Cover Crop N Calculator" (CC-NCALC), which is being used for the first time in Europe, to predict the N contribution of CCs to subsequent cash crops.

## 2 Materials and methods

### 2.1 Site description

The study area (6.5 ha) is located at the experimental farm "L. Toniolo" in Legnaro (45° 20′ 53″ N, 11° 57′ 11″ E, 6 m a.s.l.), situated in a plain region of fluvial origin in northeastern Italy (Padano Valley). The experimental site (Fig. 1) was conventionally managed since 1996 with a non-strict rotation of maize (*Zea maize* L.), wheat (*Triticum aestivum* L.), soybean (*Glycine max* (L.) Merr), sorghum (*Sorghum bicolor* L.), and sugar beet (*Beta vulgaris* L.) (Tolomio and Borin 2019) until October 2019, when the present experiment on winter CCs was instituted up to October 2022. Following the most common rotation system of the study area, maize and soybean were used as cash crops in the rotation with CCs. The soil of the experimental site is classified as Fulvi-calcaric Cambisol (WRBSR 2014). The physical-chemical characteristics (0–40-cm topsoil) are reported in Table 1, whereas the hydrological properties consisted of an upper layer saturated water content (SAT) of 45.8%, drained upper limit (DUL) of 33.9%, and permanent wilting point (PWP) of 13.4%. An impermeable layer at 3-m depth determined a shallow phreatic groundwater table fluctuating from about 0.5–1.5 m in late winter-early spring to 1.5–3 m in summer. More detailed soil hydrological properties for the soil profile down to 2-m depth are reported by Tolomio and Borin (2019).

The area is characterized by a humid subtropical climate (Cfa class in Köppen classification) (Rubel et al. 2017), and

**Table 1** Physical-chemical characteristics of the 0–40-cm soil profile at the beginning of the experiment (October 2019) from the average of 36 samples (average ± SE).

| Soil characteristics | Values |
|---|---|
| Sand, 2000–50 μm (%) | $36.9 \pm 5$ |
| Silt, 50–2 μm (%) | $44.1 \pm 5$ |
| Clay, < 2 μm (%) | $19.0 \pm 2.2$ |
| pH | $8.0 \pm 0.2$ |
| Bulk density (Mg m$^{-3}$) | $1.62 \pm 0.1$ |
| Soil organic matter (%) | $1.4 \pm 0.1$ |
| Inorganic carbon (%) | $4.25 \pm 0.2$ |
| Total Kjeldahl nitrogen (%) | $0.09 \pm 0.01$ |
| $NO_3^-$-N (mg kg$^{-1}$) | $576.6 \pm 18.1$ |

it usually has water in excess in autumn and spring and water stress in summer. Weather data (air and soil temperature, precipitation, $ET_0$) were collected from the meteorological station of the regional agency for environmental protection (ARPAV), located on the "L. Toniolo" farm. Average values for the last 30 years (1992–2022) showed annual rainfall of 830 mm and annual temperature of 13.9 °C with average minimum and maximum temperatures of 8.7 °C and 18.6 °C, respectively. The month with the lowest average minimum temperature is January (− 0.15 °C), while the month with the highest average maximum temperature is July (29.5 °C).

### 2.2 Experimental layout and crop management

Three winter CC management strategies were tested in a 3-year crop rotation with silage maize (*Zea mays* L.—in the 1st and 2nd year) and soybean (*Glycine max* L. Merr.—in the 3rd year) as cash crops. The experimental design was a



**Fig. 1** Map of the experimental site (L. Toniolo farm, Padova, Italy). The experimental design included two blocks with six plots each, where two repetitions of each of the three cover crop treatments were located (Fixed: triticale. Succession: rye in 2020, clover in 2021, mustard in 2022. NoCCs: absence of cover crops). For each plot, the Normalized Difference Vegetation Index (NDVI) was calculated from multispectral satellite images acquired by the Sentinel-2 Level 2A on 31/01/2021. Base map source: Esri, Maxar, Earthstar Geographics.
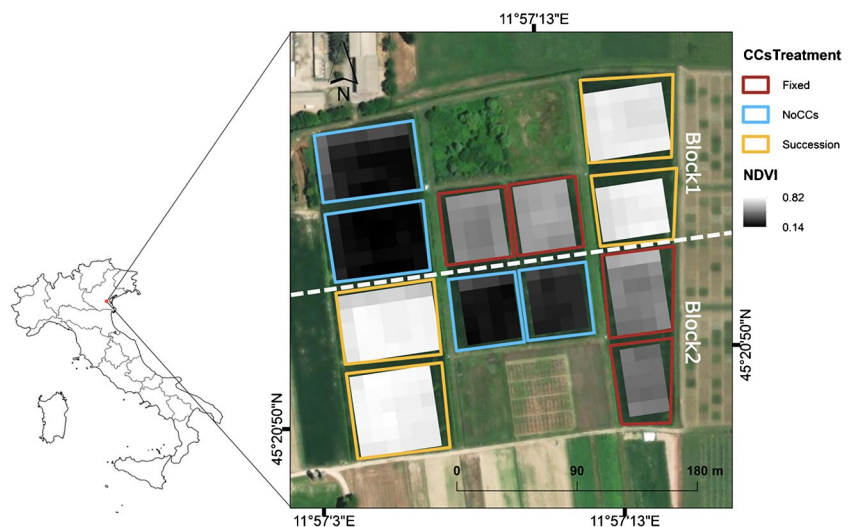
randomized split-plot including 2 Blocks and 3 CC management strategies in the main plots (Fig. 1). The 3 CC management strategies consisted of (i) a fallow treatment (NoCCs), where the soil was left bare and any chemical or mechanical operation was performed for weed control; (ii) a fixed treatment (Fixed), where triticale (X *triticosecale*) was used every year of the experimentation; and (iii) a succession treatment (Succession), where a 3-year rotation of 3 CC species was tested, including cereal rye in 2020 (*Secale cereale* L.), crimson clover in 2021 (*Trifolium incarnatum* L.), and mustard in 2022 (*Sinapis alba* L.).

The winter CCs were sowed on 10 October 2019, 9 October 2020, and 24 September 2021 with a seeding rate equal to 160 kg ha$^{-1}$ for the grasses, 40 kg ha$^{-1}$ for crimson clover, and 35 kg ha$^{-1}$ for mustard. In all the 3 years, the CCs were terminated on 31 March by shredding with a rotary mulcher for incorporating the residues. Other field operations included subsoil tillage (at 30-cm depth) after the CC termination and rolling harrow for the cash crop seedbed preparation.

The cash crops were irrigated once in 2020 (40 mm on July 12th), 2021 (30 mm on July 12th), and 2022 (40 mm on June 1st). The mineral fertilization consisted of 200 kg N ha$^{-1}$ (16% of urea before sowing and the rest as top-dressing), 80 kg P$_2$O$_5$ ha$^{-1}$, and 80 kg K$_2$O ha$^{-1}$ before sowing, for maize, and 46 kg P$_2$O$_5$ ha$^{-1}$ for soybean. Weeds were controlled, in all the 3 years, with pre-emergence herbicide application at sowing and with post-emergence mechanical control.

## 2.3 Data collection

### 2.3.1 Crop sampling

Both CCs and cash crops were sampled for their biomass production at termination and harvest time, respectively. Specifically, three samples of the CCs were collected from each main plot by hand-harvesting the aboveground biomass from 4-m$^2$ sample areas. The CC roots were sampled from a $0.5 \times 0.5 \times 0.5$ m cube of soil collected in the middle of the aboveground biomass sample area and then washed out from the soil using the method reported by Smit et al. (2013). The cash crops' aboveground biomass was collected at harvest from three sampling areas in each main plot, measuring 18 m$^2$ for the maize and 13.5 m$^2$ for the soybean.

All the biomasses were weighed for their fresh weight (FW) and then dried in a thermos-ventilated oven (65 °C) to determine dry matter content. After this, a subsample of each dry biomass was ground to pass a 2-mm sieve and analyzed for carbon (C) (only for CCs) and N contents with a CNS analyzer (CN 802 Carbon Nitrogen Elemental Analyzer, Velp Scientifica, Usmate, Italy).

### 2.3.2 Soil water content sampling

The soil water content (SWC), sampled in each plot, was measured on a weekly basis ($\pm$ 4 days) every 10 cm from 0 to 100-cm depth using Sentek's Diviner2000 capacitance sensor (Sentek Environmental Technologies, Kent Town, South Australia). The sampling campaign for the SWC was performed during the CCs growing seasons (from October to March in 2020–2021 and 2021–2022) and the cash crop growing cycle (from June to October 2020, from April to October 2021, and from April to September 2022). The SWC content time-series values were reported for both CCs and cash crop seasons, as the difference between each value measured in each sampling date and the initial ($t = 0$) value measured at the beginning of each growing season (Table 1S).

### 2.3.3 Sentinel-2 measurements

A time series of multispectral satellite images collected by the Sentinel-2 Level 2A over the experimental site was downloaded from the European Space Agency (ESA) DataHUB server (ESA 2022). For each image, it was visually confirmed that the absence of cloud and cloud shadow over the experimental site. This process resulted in a total of 10 images for each CCs growing season (11 and 26 October, 10 November, 5 and 25 December 2019; 9 and 24 January, 8 and 28 February; 19 March; 10 and 25 October; 24 November 2020; 8 and 14 January, 17 February, 9 and 24 March; 10, 15 and 30 October, 24 November 2021; 8 and 18 January; 2 and 12 February; 9 and 24 March 2022). The Sentinel-2 payload is the Multi-Spectral Instrument (MSI) that measures the radiation reflected from the Earth in 13 spectral bands: four bands at 10-m, six bands at 20-m, and three bands at 60-m spatial resolution (Table 2S). The bands registered reflectance in the visible, red edge and NIR regions at 10- and 20-m spatial resolution were extracted from the pixels that completely lay within each plot. The number of pixels ranges from a minimum of 15 to a maximum of 36 per plot (Fig. 1). The extracted bands of each image were used to calculate various VIs related to different agronomical variables to test their potential for monitoring CC growth and performance (Table 2). This study tested the performance of three VIs based on the visible and NIR (NDVI, GNDVI, and SAVI) and one that incorporates a band from the red-edge region (NDRE) as reported in Table 2. The QGIS software (QGIS Development Team 2020) version 3.28.1. was used to extract the spectral bands. The R software (R Core Team 2021) was used to calculate the VIs of each date.

## 2.4 CC-NCALC model

The expected N mineralization (or immobilization) from CC residue decomposition was estimated through a web-based

**Table 2** The equations and the equations adapted to the multispectral Sentinel-2 bands of the vegetation indices used in this study.

| Index | Equation | Equation Sentinel-2 | Reference |
|---|---|---|---|
| Normalized Difference Vegetation Index (NDVI) | (R800 − R670)/(R800 + R670) | (B8 − B4)/(B8 + B4) | Rouse et al. 1974 |
| Green NDVI (GNDVI) | (R800 − R550)/(R800 + R550) | (B8 − B3)/(B8 + B3) | Gitelson et al. 1996 |
| Soil-Adjusted Vegetation Index (SAVI) | (1 + 0.5) * (R800 − R670)/(R800 + R670 + 0.5) | (1 + 0.5) * (B8 − B4)/(B8 + B4 + 0.5) | Huete 1988 |
| Normalized Difference Red Edge (NDRE) | (R790 − R720)/(R790 + R720) | (B8 − B6)/(B8 + B6) | Barnes et al. 2000 |

model called "Cover Crop N Calculator" (CC-NCALC) developed by the University of Georgia (Woodruff et al. 2018; Thapa et al. 2022). The model, described in detail by Woodruff et al. (2018), is a modified and implemented version of the N mineralization and immobilization subroutine from the CERES-N model (Godwin and Allan Jones 1991). It focuses on the decay of the fresh organic matter of the CC residues to calculate the corresponding N accounting and estimate the amount of inorganic N mineralized (or immobilized). The model uses as input data: (i) the dry CC biomass yield and the composition of the CC residues including the fresh matter components (nonstructural carbohydrates, cellulose, and hemicellulose, and lignin) and the C:N ratio; (ii) agricultural management information about the CC sowing and termination time, the management of the residues (incorporated or left on the surface), the type of the agricultural systems (organic or conventional), the cash crop cultivated after the CCs season, and the usual quantity of N fertilizer applied; (iii) environmental parameters such as the daily 0–30 cm SWC and the soil 10 cm temperature for the decomposition period to be simulated, the soil hydrological characteristics (LL, DUL, SAT), the BD, the soil organic carbon content (SOC), and inorganic N.

In the present study (for each of the 3 experimental years), the meteorological data and the soil 10 cm temperature were collected by a weather station located at the experimental site (Vantage Pro Meteo Station by WeatherLink). The 0–30 cm SWC was measured in the experimental field as described in Section 2.3, and the BD and the SOC, as well as inorganic N, as reported in Raimondi et al. (2023). The CCs' biomass C, N, and water contents were determined, for each experimental year, as reported in Section 2.3.1, whereas the fresh organic matter components were estimated using the following equations (R. Thapa, personal communication):

$$\%Carbohydrate = 24.7 + 10.5 * \%N \qquad (1)$$

$$\%Holo-cellulose = 69 - 10.2 * \%N \qquad (2)$$

$$\%Lignin = 100 - \%Carbohydrate - \%Holo-cellulose \qquad (3)$$

The model output gives the cumulative amount of N mineralized (kg N ha$^{-1}$) (from now on referred to as N release)

from the CCs residues over the following cash crop season (140 days in the present study. In addition, it explains how the output N release (kg ha$^{1}$) estimated by the model can be used to adjust the N fertilization rate.

## 2.5 Statistical analysis

Descriptive statistics were computed for all the datasets to analyze the main feature of the data distribution. Two analysis procedures were used in the present study to analyze: (1) the cash crops and CCs performances (dry biomass quantity, N uptake, C/N ratio) and the total N released by CCs residues among the different treatments in all 3 years of the experimentation; (2) the SWC during both the CCs and the cash crop season, the VI trend during the CCs growing season, and the N release rate from CC residues (calculated using the slope of lines fitted on monthly N release data) in each year of the experimentation. Marginal and conditional residual distributions were visually checked to detect possible issues of non-normality or heterogeneity of variances, for each analysis performed. The first analysis was performed using linear mixed models ("lmer()" function in R software) (Bates et al. 2015) including the CC treatments and the year as fixed factors and the block as a random effect (Onofri et al. 2016). The second analysis consisted in investigating the temporal trends of the variables using a generalized least squares (GLS) fitting procedure to estimate the standard error accounting for the autocorrelation in the residual series (Cowpertwait and Metcalfe 2009; Campi et al. 2019). Using the gls() function (within the nlme library) on R software, models for repeated measures were built including the CCs treatments as fixed effects. The sampling dates were included in the models as repetition factors, and they were specific for each outcome variable: (i) 2 weeks for the SWC values; (ii) months for VI measurement; and (iii) months for the N release rate by the CCs residues. In addition, simple linear models for repeated measures were also computed for each variable including the same fixed effects. After fitting all the models, the Akaike Information Criterion (AIC) was used to assess and identify the one best fitting the datasets. For all the statistical procedures performed, a Wald test ANOVA of the best-fitting models was used to confirm the

sources of variation, and post hoc analyses were carried out with the Sidak test for multiple sets of pairwise comparisons or Tukey test for one set of pairwise comparisons (Lenth et al. 2021). To assess the correlations among the VIs and both CC biomass and N uptake, their Spearman's rank correlation coefficients were computed using the R function "cor" with option method = "spearman." Heatmaps depicting the matrix of Spearman's rank correlation coefficients within each experimental year were then created with R package "gplots." All the statistical analyses were performed with R software (R Core Team 2021).

# 3  Results

## 3.1  Meteorological data

For all the experimental years, the yearly rainfall (Fig. 2) was lower than the 30-year average (830 mm) with 701 mm in 2020, 630 mm in 2021, and 464 mm in 2022. The cumulative rainfall registered during the CC season, showed a total of 380 mm in 2020, 279 mm in 2021, and 175 mm in 2022. From October to March, an increase in rainfall events occurred in 2020, while a decreasing pattern was registered in 2021 and 2022. In 2020, the highest cumulative value was registered in March (60 mm), while in 2021 and 2022 the highest precipitation was measured in January and December with 72 and 36 mm, respectively. During the cash crop season, the highest concentration of precipitation events was registered in June and August 2020 (158 mm on average), May 2021 (132 mm), and August and September 2022 (84 mm on average).

The highest and lowest air temperatures were measured in July/August and January for all the experimental years, confirming the pattern observed in the last 30 years. However, the yearly average maximum (25 °C) and minimum (3 °C) temperatures registered during the experimental period were 3.4 and 2.8 times higher than the average 30-year

values, respectively. The soil temperature over the 3 years followed the same pattern as the air temperature, with an average maximum value equal to 25 °C in July, and a minimum temperature of 4.6 °C in January. In the summer season (June–August) of both 2020 and 2021, an average soil temperature of 24.3 °C was registered, whereas the air temperature was equal to 23.4 °C (on average). In the summer season of 2022, the soil and air temperatures were equal to 24.1 and 25.5 °C, respectively. During the autumn and winter seasons of all the experimental years, the soil temperature (9.3 °C on average) was slightly higher than the air temperature (8.4 °C). The ET0 distribution showed the lowest values from November to January in all the years of the experimentation, while the highest was between June and July months.

## 3.2  Cover crops' growing season

### 3.2.1  Vegetation indices for cover crop monitoring

The temporal evolution of the VIs during the CC season of the 3 experimental years (Fig. 3) showed different patterns depending on the year, the treatment, and their interaction (Table 3S). All the VIs resulted positively correlated with each other's in all experimental years, with Spearman's rho values ranging from 0.73 to 0.99 (Fig. 4). The values of the VIs based on the visible and NIR increased during the first months of all three CCs growing seasons. Differently, the temporal profiles of the VIs in the last months before CC termination differed among years. In 2020 and 2021, the VIs maintain or increase their value until the end of the CCs, whereas, in 2022, the NDVI, GNDVI, and SAVI decreased abruptly in February due to the frost damage suffered by the CCs. Overall, the VIs based on the visible and NIR allowed to discern more the differences among treatments compared to the (NDRE). Particularly, the NDVI displayed the biggest differences between CC treatments, especially when distinguishing between the Fixed and the NoCCs treatment. The identification of the succession treatment varied between years.

**Fig. 2** Monthly rainfall (mm), irrigation (mm), and ET0 (mm) and mean air and soil temperature (°C) during the experimental period at L. Toniolo experimental farm (Padova, Italy).
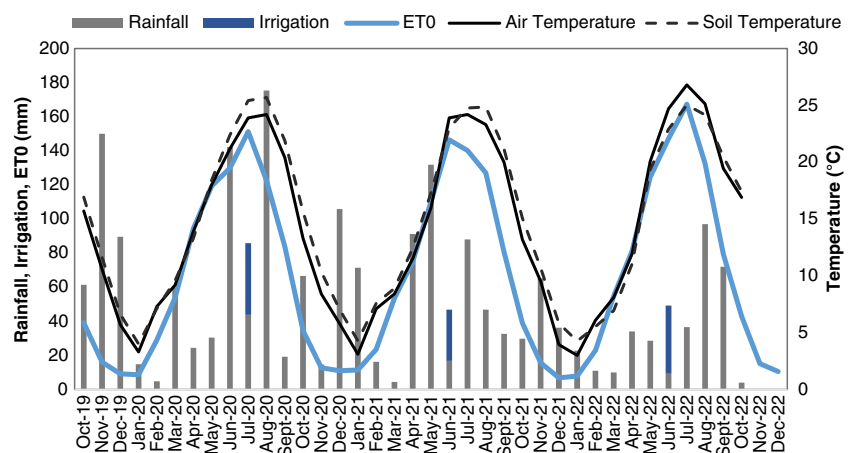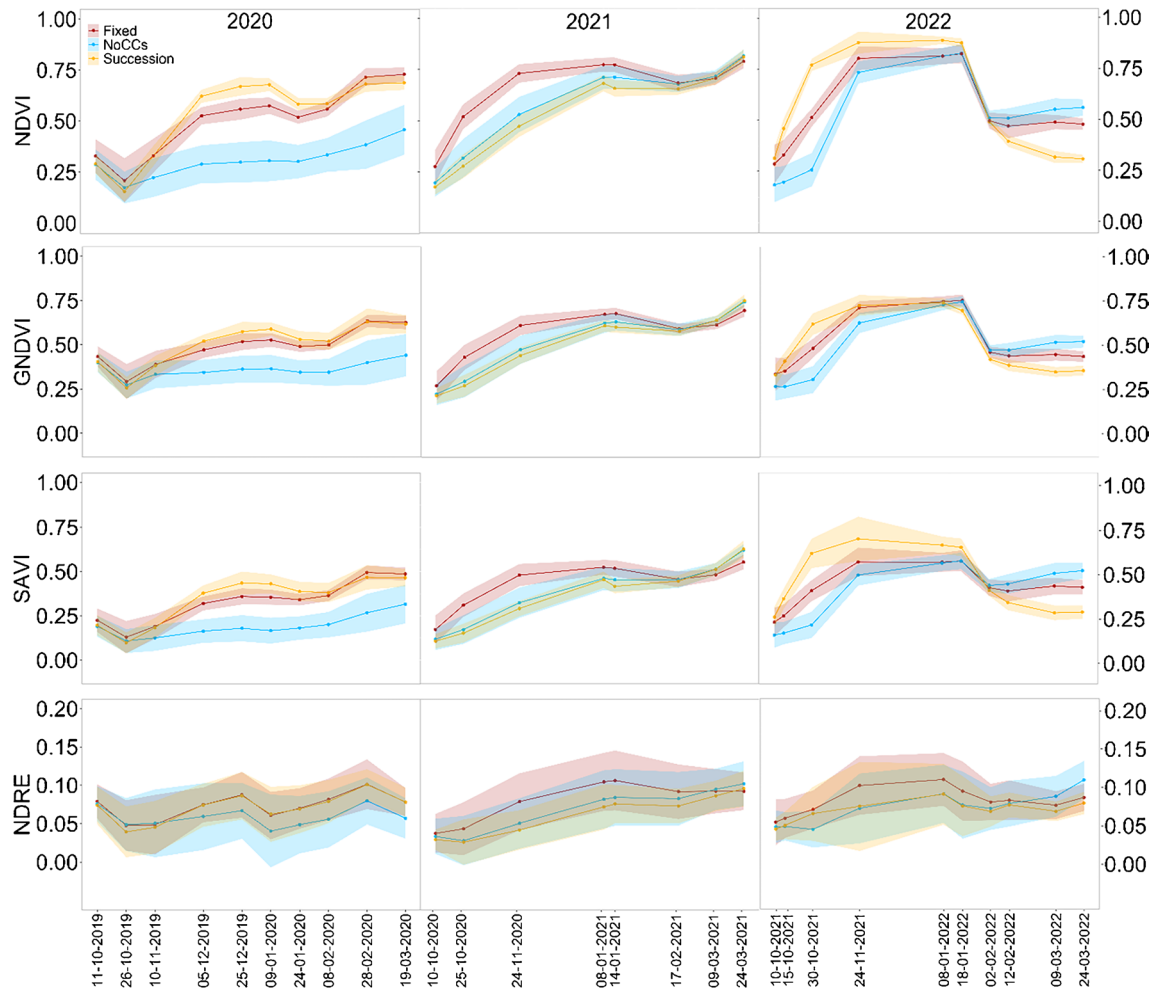
**Fig. 3** Temporal evolution of NDVI, GNDVI, SAVI, and NDRE calculated from Sentinel-2 imagery from the experiment for each cover crop treatment (Fixed: triticale. Succession: rye in 2020, clover in 2021, mustard in 2022. NoCCs: absence of cover crops) during the three growing seasons. The points represent the date of image acquisition, the ribbon, and the standard error.

The robustness of the NDVI for CC biomass monitoring was strengthened by the significant relationship with biomass registered at the termination date of the 3 years (Fig. 4). In all cases, Spearman's rho values of NDVI varied between 0.56 and 0.77, even in 2021, when the other VIs' analysis did not correlate with biomass, and only NDVI and GNDVI obtained a moderate correlation. In 2020 and 2022, the NDVI obtained a significant correlation with biomass ($p < 0.01$). A significant correlation between all VIs and N uptake at CC termination was found in 2020, with the highest value obtained by the NDRE (Spearman's rho = 0.71). In 2022, only the NDVI positively correlated with CCs N uptake (Spearman's rho = 0.51).

The highest differences of the VIs based on visible and NIR were observed between both the treatments with CC (Fixed and Succession) and the NoCC treatment in the first experimental year from 5 December 2019 to the termination date (March 19th 2020). The NDVI and SAVI values of both fixed and succession treatments were almost double the NoCC values, while GNDVI values were ≈ 50% higher for both treatments compared to the NoCC treatment. Rye and triticale throughout the first experimental season always showed the same values of all the VIs, except for 3 dates between the end of December and the first of January when rye showed higher NDVI compared to triticale.

In the 2021 growing season, from the end of October to the end of November, all three VIs based on the visible and NIR were significantly higher in the fixed treatment compared to the other two treatments. However, NDVI and SAVI were those displaying the biggest differences between fixed and the other CCs treatments. Higher NDVI values were found for triticale, compared to crimson clover and NoCCs, until the half of February. Any significant difference among treatments was registered in the NDVI from the half of February till the CC termination (end of March). Particularly, triticale NDVI values were 58.8% and 64.9%

higher than both clover and the spontaneous vegetation (No CCs) on October 25th (0.3 on average) and November 24th 2020 (0.5 on average), respectively. While the GNDVI was 40% and 25% higher in the triticale treatment compared to NoCC on October 25th and November 24th. At the end of January 2021, NDVI was equal to 0.7 for triticale and 0.6 for both succession (crimson clover) and NoCCs. From the half of February, the NDVI was equal in all the treatments with average values of 0.6 on February 17th, 0.7 on March 9th, and 0.8 on March 24th 2021. SAVI followed a similar pattern to NDVI but with lower values. This difference between the two indices increased with the growing season as it was < 0.1 at the beginning of October to ≈ 0.2 at the termination date.

Similar to 2021, in the 2022 growing season, the biggest differences between treatments were found in the last two dates of October, with significant differences between Fixed and NoCC treatments in all VIs based on the visible and NIR. However, SAVI and NDVI also displayed significant differences between Succession (mustard) and Fixed (triticale) treatments. In 2022, mustard showed the highest NDVI values until the first days of January, compared to both triticale and NoCCs. On February 2nd 2022, the NDVI values in all the CC treatments showed a significant drop reaching the same value of 0.5 in all the treatments. From this date until the CC termination, triticale and the spontaneous species always showed higher NDVI compared to the mustard. Specifically, on February 12th 2022, the NDVI values were 0.5 for triticale and NoCCs and 0.3 for mustard. On March 9th and 24th 2022, the spontaneous species in the NoCCs showed the highest NDVI values (0.5 and 0.6, respectively), followed by triticale (0.4 on both dates) and mustard (0.3 on both dates). As observed in 2021, SAVI followed a similar pattern to NDVI, and the differences between SAVI and NDVI increased across the growing season, starting from a difference of < 0.1 in October and reaching the biggest difference on January 18th 2022. However, in 2022, after reaching the highest difference, it was reduced to < 0.7 on the termination date on March 24th 2022.

Overall, the VI based on the red-edge region (NDRE) presented an increasing tendency during the growing season of all CC treatments and years but exhibited some reduction of the values in certain winter dates. In 2020, a reduction in NDRE was observed for all CC treatment on December 25th 2019. This reduction was registered 2 weeks before the reduction experienced by the VIs related to green biomass (January 9th 2021) in the triticale and rye treatments (no reduction was observed in the NoCCs treatment in the green biomass VIs). The reduction of NDRE in 2021 started on the same date as the reduction of the VIs related to green biomass (January 14th 2021). However, the reduction in NDRE was only registered by the triticale treatment while the other treatments only showed a decline in the increasing tendency.

The reduction in NDRE observed in the 2022 winter dates by all CC treatments was registered 10 days (January 8th 2022) before the decrease observed in the VIs related to green vegetation.

### 3.2.2 Soil water content

All the SWC values during both the 2020–21 and 2021–22 winter seasons (Fig. 5) showed significant variable trends in time (Table 4S). In the third experimental year, the SWC in both 0–50 and 50–100 layers was also significantly affected by the CC treatment (Table 4S). All the results of post hoc analyses are reported in Tables 4S to 7S. All the SWC values from here on are reported as the positive or negative difference (+ or −) from the initial ($t = 0$) SWC measured at the beginning of each growing season (Table 1S).

In the second and third winter seasons, despite different rainfalls registered (279 mm in 2020–21; 175 mm in 2021–2022), no SWC increase was observed between the CCs sowing and termination time. The winter rainfall allowed to reach field capacity (FC) by January (in both years) in the 0–50-cm depth but not in the deeper soil layer (50–100-cm depth).

Specifically, in the 2020–21 winter season, the highest SWC content values for the first 0–50-cm depth were registered at the end of January and the first days of February. An average of + 34 mm was measured from January 29th to February 3rd 2021, whereas the highest value was registered on February 11th 2021 (+ 39.4 mm). The lowest SWC values were measured both at the beginning and the end of the winter season. On November 12th, the lowest value of − 0.2 mm was registered, while on average + 4.6 and + 22.6 mm were measured from October 28th to November 26th and from March 5th to 25th, respectively. On the deeper soil layer (50–100-cm depth), in 2020–21, after the lowest SWC values (+ 0.19 mm) measured from October 20th to December 4th 2020, an increasing trend was observed until February. In January, higher values (+ 29.3 mm) were registered, before reaching the highest average values of + 47.5 mm in February. Similar values to January were registered in March.

In the 2021–22 winter season, the SWC content in the upper soil layer was significantly higher in the NoCC treatment (+ 37.3 mm on average) compared to the succession (+ 31.6 mm on average), whereas the fixed treatment (35.2 mm on average) did not show any significant difference from the other two. In the 50–100-cm depth, differently, the SWC content measured in both NoCCs and fixed treatments was significantly higher than the succession. Looking at the SWC trend in time for the 0–50-cm layer, it can be observed that the highest average values of + 44.5 mm were measured from the end of December till the end of January. The lowest values were observed at the beginning

**Table 3** Total CCs' (aboveground and belowground) dry biomass weight (Mg ha$^{-1}$) (DB), N content (kg ha$^{-1}$), C/N ratio, N release accumulation (% of cover crops dry biomass total N uptake—kg ha$^{-1}$), biomass carbohydrate (%), holocellulose (%), and lignin (%) content of each cover crops treatment at termination time of each year of the experimentation (2020; 2021; 2022) * significance ($p$ value < 0.001); $ns$, not significant (Wald test ANOVA).

| Year | Treatment | CC DB (Mg ha$^{-1}$) | CCs' total N uptake (kg ha$^{-1}$) | CCs' total C/N | Total N release (%) | Carbohydrate (%) | Holocellulose (%) | Lignin (%) |
|---|---|---|---|---|---|---|---|---|
| 2020 | NoCCs | 1.2e | 17.6 d | 19.8 de | 11.8 | 39.2 cd | 54.8 cd | 5.8 |
| | Succession (rye) | 7.6 a | 90.7 ab | 28.1 bc | 11.9 | 37.2 de | 56.8 bc | 5.9 |
| | Fixed (triticale) | 6.6 ab | 73.7 abc | 28.6 abc | 4.5 | 36.1 ef | 57.9 ab | 5.9 |
| 2021 | NoCCs | 4.2 cd | 80.9 abc | 19.2 e | 28.4 | 43.9 ab | 50.2 ef | 5.7 |
| | Succession (clover) | 3.7 d | 64.5 c | 19.9 de | 38.2 | 45.1 a | 49.1 f | 5.7 |
| | Fixed (triticale) | 5.3 bcd | 66.4 bc | 27.2 bc | 15.6 | 36.5 def | 57.5 abc | 5.9 |
| 2022 | NoCCs | 6.9 ab | 98.3 a | 25.1 cd | 15.6 | 38.3 de | 55.7 bc | 5.9 |
| | Succession (mustard) | 7.5 a | 84.1 abc | 31.2 ab | 28.1 | 42.1 bc | 52.1 de | 5.8 |
| | Fixed (triticale) | 5.7 abc | 62.7 c | 34.0 a | -8.8 | 34.1 f | 59.9 a | 6.0 |
| Treatment | | ns | ns | ns | * | * | * | ns |
| Time | | ns | ns | ns | ns | ns | ns | ns |
| Treatment × time | | * | * | * | ns | * | * | ns |
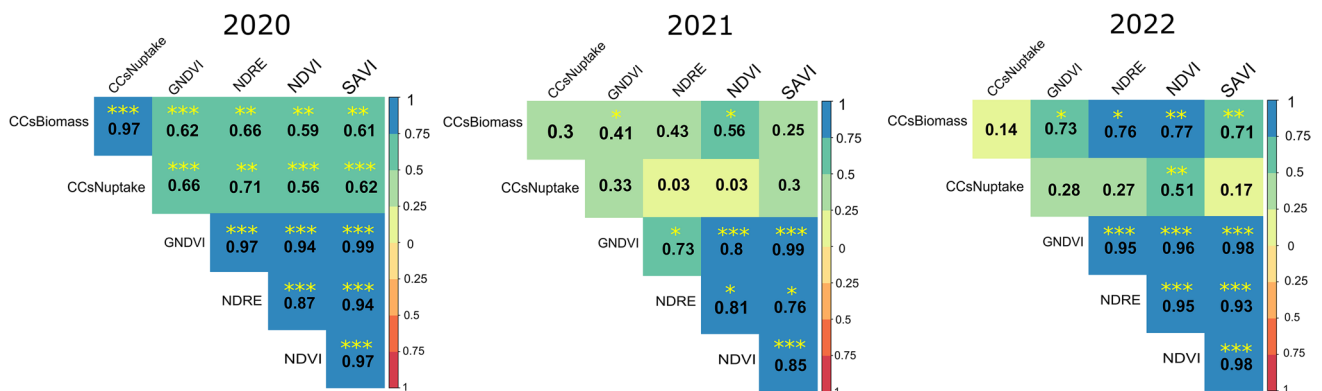


**Fig. 4** Spearman correlation heatmap between vegetation indices (GNDVI; NDRE; NDVI; SAVI) and cover crop total (aboveground and roots biomass) biomass production (CCsBiomass) (Mg ha$^{-1}$) and N uptake (CCsNuptake) (kg ha$^{-1}$). Statistical differences are marked with * ($p < 0.05$), ** ($p < 0.01$), *** ($p < 0.001$). $R$-values are displayed in different colors, as indicated by the color code on the right side of the heat map.

of the winter season on October 21st (+ 8.26 mm) and at the end of March (+ 25.5 mm). For the 50–100-cm depth, the SWC trend showed the highest values (+ 22.6 mm on average) from the first days of January till the half of March, and the lowest values (+ 4.7 mm on average) only at the beginning of the season from October 21st until December 7th.

The analysis of the SWC at CC termination time showed any significant difference among treatments in both winter seasons (2020–21; 2021–22) except for the values registered in the fixed treatment at the 50–100-cm depth (+ 37.2 mm), higher than both the NoCCs and the succession (18.6 mm).

## 3.3 Cover crop effect during the cash crop season

### 3.3.1 Cover crops' residues quality and N release

The CCs' dry biomass quantity and quality (N uptake-kg ha$^{-1}$, and C/N ratio) (Table 3) in the present study were significantly affected by the interaction between the CC treatment and the year. Both the succession treatments of the first (cereal rye) and last (mustard) years of experimentation showed the highest dry biomass (7.5 Mg ha$^{-1}$ on average), whereas the lowest value was observed in the succession treatment of 2021 (3.7 Mg ha$^{-1}$ for crimson clover). All the

**Fig. 5** Average soil water content (SWC) (mm) in the 0–50 and 50–100 cm layers, for the winter season of both 2020–2021 and 2021–2022. Different letters indicate significant differences ($p < 0.01$) among treatments (Fixed: triticale. Succession: rye in 2020, clover in 2021, mustard in 2022. NoCCs: absence of cover crops) in the SWC values measured the last day before the CCs termination (29/03) in both the 2021 and 2022 years. ns: no significant difference among treatments ($p < 0.01$). The standard error is represented by the ribbon around the lines.
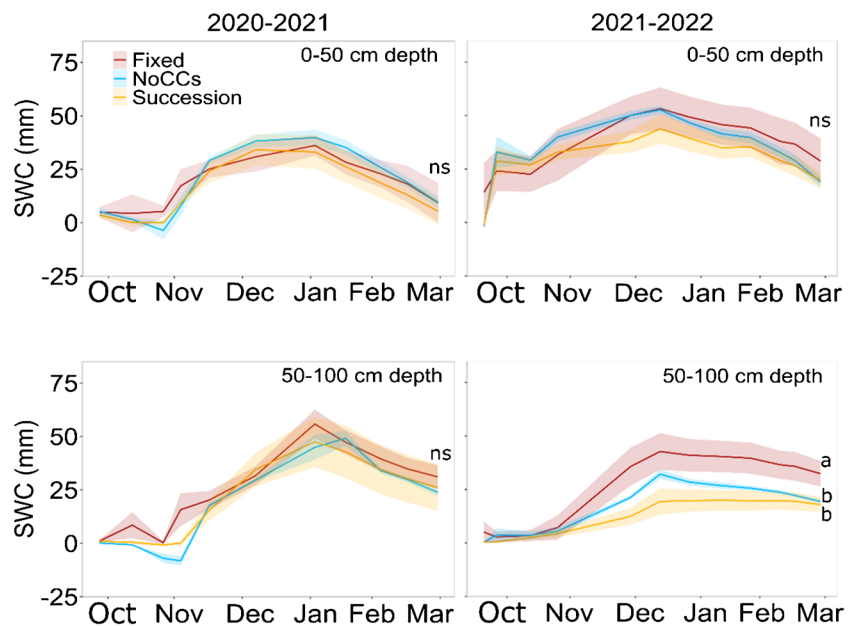


other treatments showed intermediate values. The succession and the fixed treatments of 2020 along with the NoCCs of 2021 and 2022 and the succession of 2022 showed the highest total N uptake (85.5 kg ha$^{-1}$ on average) at termination time (March). The fixed treatment of both 2021 and 2022 and the succession treatment of 2021 showed in-between values, while the NoCCs of the first experimental year registered the lowest value (17.6 kg ha$^{-1}$). Differently, the C/N ratio was higher in the fixed treatment of both the last and the first experimental year and in the succession of 2022 (31.2 on average). The NoCCs of 2020 and 2021 along with the succession treatment of 2021 registered the lowest C/N ratios (19.6 on average), while the rest of the treatments were in-between.

The curves in Fig. 5A, C showed the estimated cumulative daily total N release (kg ha$^{-1}$ day$^{-1}$) coming from both the aboveground and root biomass residue decomposition over the whole cash crop growing season in 2020, 2021, and 2022. All the total N release curves showed nonstationary trends in time affected by the CCs treatment and by the interaction of the two variables, except for the roots biomass of 2020 which was only affected by the CC treatment (Table 9S).

With regard to the monthly N release rate (kg ha$^{-1}$ month$^{-1}$) of each treatment in comparison with the others in each experimental year (Fig. 6B, D), it can be noticed that all the N release rates from both the aboveground and root biomass in all the experimental years were affected by the interaction between the time and the CCs treatment, except for the root biomass in 2020 and 2021, that were equal between treatments and constant in time (Table 10S). All the results of the post hoc analyses are reported in Tables 11S to 16S. In 2020, the succession treatment (rye

species) showed an increasing pattern from April (0.04 kg ha$^{-1}$ month$^{-1}$) until June, when it reached the highest N release rate (0.08 kg ha$^{-1}$ month$^{-1}$). From June, a decreasing rate was registered in the succession treatment until July when it reached the same lower values of both fixed treatment and the NoCCs (0.01 kg ha$^{-1}$ month$^{-1}$). From August until the cash crop termination, the same lowest N release rate was registered in all the treatments (0.005 kg ha$^{-1}$ month$^{-1}$ on average).

In 2021, the highest N release rate (0.28 kg ha$^{-1}$ month$^{-1}$) from the aboveground biomass was measured in the NoCCs and the succession treatment (crimson clover) in April and May, followed by the values registered for the same treatments in June (0.13 kg ha$^{-1}$ month$^{-1}$), in July (0.04 kg ha$^{-1}$ month$^{-1}$) and at the end of August where the lowest values were registered (0.02 kg ha$^{-1}$ month$^{-1}$). The N release rate in the fixed treatment instead showed the same values registered in the NoCCs and succession treatment in June, already at the beginning of the season in April, keeping similar values until June, when it reached the lowest values until the end of August. In this month, all treatments registered the lowest N release rate of the season, equal to 0.02 kg ha$^{-1}$ month$^{-1}$.

The aboveground biomass in 2022 instead showed the highest N release rate in the NoCC treatment in April and May (0.27 kg ha$^{-1}$ month$^{-1}$) followed by the succession treatment in the same months and the NoCCs in June (0.16 kg ha$^{-1}$ month$^{-1}$). Starting from June, for the succession treatment, and from July for the NoCC treatments, the lowest N release rates were measured (0.04 kg ha$^{-1}$ months$^{-1}$) until the end of August. The same lowest value (0.04 kg ha$^{-1}$ month$^{-1}$) was measured in the fixed treatment from April throughout the entire summer season.

**Fig. 6** Daily total N release (kg ha$^{-1}$ day$^{-1}$) (**A–C**) and monthly N release rate (kg ha$^{-1}$ month$^{-1}$) (**B, D**) from both aboveground (AB) and roots (RB) cover crop residues during the summer seasons of each experimental year (2020; 2021; 2022) (Fixed: triticale. Succession: rye in 2020, clover in 2021, mustard in 2022. NoCCs: absence of cover crops). The standard error is represented by the ribbon around the lines.
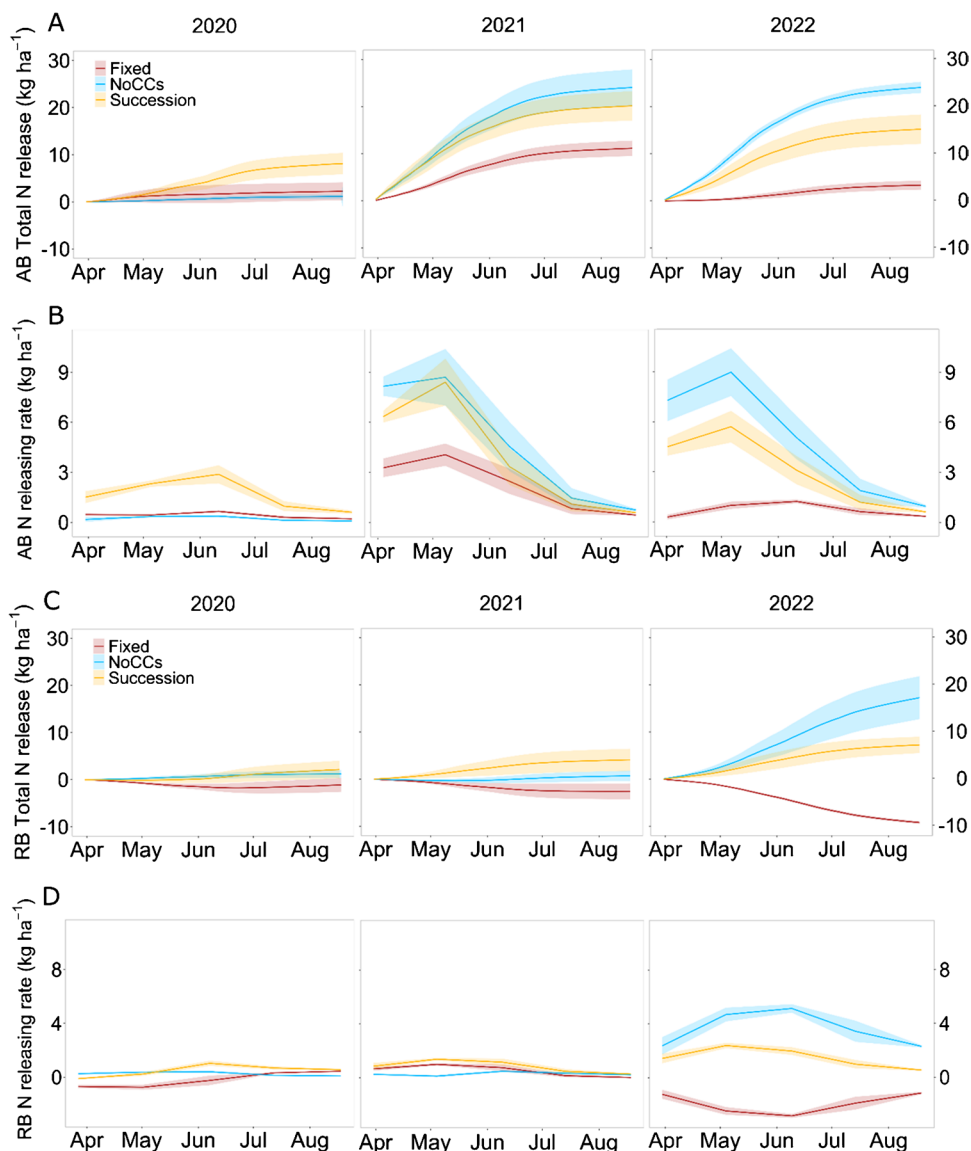
The N release rate from the roots biomass in 2022, showed the highest value in the NoCC treatment in May and June (0.16 kg ha$^{-1}$ month$^{-1}$) followed by the values in the NoCCs in April, July, and August, and the succession treatment in May (0.09 kg ha$^{-1}$ month$^{-1}$). An average value of 0.04 kg ha$^{-1}$ month$^{-1}$ was measured in the succession treatment in April, June, July, and August. In the fixed treatment, the lowest values compared to all the other treatments were registered from April to June ($-$ 0.08 kg ha$^{-1}$ month$^{-1}$), whereas in July and August, there was a slight increase ($-$ 0.03 kg ha$^{-1}$ month$^{-1}$) even if the values were still lower than the other two treatments.

The analysis of total cumulative N release during the summer season (Table 3) expressed as a percentage of cover crops dry biomass total N uptake (kg ha$^{-1}$) showed that it was significantly affected only by the CC treatment. The succession treatment had a higher value (26.1% on average) compared to the fixed (3.7% on average) with the NoCCs showing any significant differences (18.6% on average). The CC residue quality differed for their carbohydrate and holocellulose content percentage according to the CC treatment in interaction with the year, whereas the lignin content did not show any significant difference. The highest percentages of carbohydrates were found in the succession treatment and the NoCCs of 2021, whereas the lowest values were in the fixed treatments of all the years of experimentation (2020, 2021, 2022). The succession treatment and the NoCCs of 2020 and 2022 showed intermediate carbohydrate contents. An opposite result was observed for the holocellulose content where the highest values were registered in the fixed treatment in all three experimental years (2020, 2021, 2022), and the lowest values in both succession and NoCCs treatment in 2021. Intermediate holocellulose contents were observed in the succession treatment of both 2020 and 2022 and the NoCCs 2020.

INRA𝒆  Springer

### 3.3.2 Soil water content

SWC during the three cash crop seasons (Fig. 7) showed variable trends in time, and only in 2021 and 2022, the SWC in both 0–50 and 50–100 cm was also affected by the CC treatment (Table 17S). The results of all the post hoc analyses are reported in the supplementary materials (Table 18S to 23S). All the SWC values from here on are reported as the positive or negative difference (+ or −) from the initial (t = 0) SWC measured at the beginning of each growing season (Table 1S).

In 2020 and 2022 years, the SWC showed low variation from the cash crop sowing to the harvest time. In the first year, around + 27 mm of SWC (0–50 and 50–100 cm depth average of all the treatments) were registered at the beginning of the cash crop season and a total of 435 mm of rainfall were observed over the summer period. In 2022, cumulative rainfalls of 277 mm were measured over the cash crop growing season, and around − 6.3 mm of SWC (0–50 and 50–100 cm depth average of all the treatments) were registered at soybean sowing time (Fig. 7). In 2021, intermediate conditions in terms of rainfall were observed for the summer period (total of 407 mm), and the SWC showed a decreasing pattern in all the treatments from the cash crop sowing date and the harvest time (Fig. 7).

Specifically, in 2020, a similar pattern of SWC values was observed in both 0–50 and 50–100-cm depths. The highest SWC values were registered at the half and end of June (June 12th and 22nd 2020) (+ 31 and + 18 mm for the upper and deeper soil layers, respectively). In July, the SWC content in the upper 0–50 cm reached the lowest values, similar to the end of the season (September 30th and October 7th 2020) (− 0.39 mm), before increasing again in August reaching 13.3 mm. In the deeper soil layer, the lowest SWC values (− 13.3 mm) were reached from the half of July (July 14th 2020) and kept constant till the end of the season (September 30th 2020).

In summer 2021, the SWC in both the soil depths 0–50 and 50–100 cm, resulted significantly higher in the NoCC treatment (− 0.3 and − 3.7 mm in the upper and deeper layers, respectively) compared to the succession treatment (− 5.5 mm in 0–50-cm depth and − 9.1 mm in 50–100-cm depth) which was also higher than the fixed treatment (− 18.4 and − 16.9 mm in the upper and deeper layers).

The SWC values in 2021 were also significantly different over the season in both 0–50 and 50–100-cm depth. In the upper soil layer, the highest SWC values were measured in the half of April and half of May (+ 31 mm), whereas the lowest (− 45.1 mm) were in September. Average values of − 5.7 mm were observed in June and the first half of July, whereas − 26 mm on average were registered at the end of July and the first days of October. In the 50–100-cm depth, the highest value (+ 40.1 mm) was registered on May 26th 2021 followed by the values measured on May 14th and 20th 2021 (+ 17.3 mm). The lowest values were measured from the half of August until the first of October (− 40.4 mm), whereas average values of − 10.9 mm were measured from the end of June until August.

In 2022, the SWC values in both 0–50 and 50–100-cm depths were affected by the different CCs treatment showing higher values in both NoCCs and fixed treatment (− 10.9 mm in the upper soil layer and − 7.5 mm in the deeper soil layer) compared to the succession treatment (− 31 and − 19 mm in the upper and deeper soil layers). During the summer season, the highest values in the upper soil layer were registered on April 28th and June 9th 2022 (− 5.3 mm), while the lowest was on the first days of September (− 40.1 mm). The nonconstant trend during the summer season revealed an average SWC of − 13.2 mm in May, half of June, and July. An average of − 18 mm was registered at the end of June, July, and end of August. In the deeper soil layer, the SWC in 2022 showed the same highest average value of − 6.8 mm from April to the second half of July, followed by an SWC of



**Fig. 7** Average soil water content (SWC) (mm) in 0–50 and 50–100-cm depth for the summer season of 2020, 2021, and 2022. Fixed treatment: triticale; Succession treatment: rye in 2020, clover in 2021, mustard in 2022; NoCCs: absence of cover crops). The standard error is represented by the ribbon around the lines.
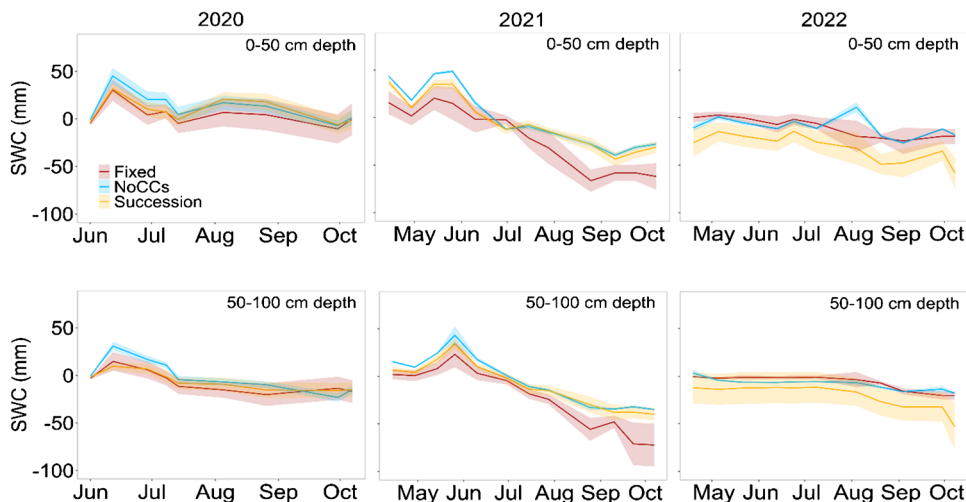
− 19.9 mm registered at the end of July and the whole month of August. The lowest value of − 36.8 mm was registered on September 7th 2022.

### 3.3.3 Cash crop performance

The cumulative marketable dry biomass production over the three experimental years (Fig. 8) did not show any significant difference among the three treatments with an average value of 11.9 Mg ha$^{-1}$. Similar results were found for the total cumulated N uptake in the cash crop dry marketable biomass (181.2 kg ha$^{-1}$ on average).

## 4 Discussion

Cover crops growing dynamics can be detected by VIs calculated through satellite images (Kariyeva and Van Leeuwen 2011, Fan et al. 2020). Among the VIs analyzed in this study, the NDVI showed the most robust results for CC monitoring because it was the only vegetation index that presented a significant correlation with CCs biomass all years at the termination date and displayed the most optimal temporal profile, emphasizing differences between CCs treatments. The NDVI has been indeed widely used for assessing vegetation evolution and detecting the percentage of ground cover by the winter CCs (Thieme et al. 2020).

In our study, triticale and rye presented a similar pattern in 2020, both showed rapid growth, reaching an NDVI ≥ 0.5 already in December, confirming previous results showing their potential for removing soil inorganic N and reducing the risk for nitrate leaching (Ruffo and Bollero 2003). However, the faster increase in NDVI, GNDVI, and SAVI values observed for rye suggested a greater biomass production than triticale in December and January, despite the same biomass measured at termination. The result confirmed the rye and triticale biomass production measured in January and in March reported in Raimondi et al. (2023). Similar results were observed in previous studies (Prabhakara et al. 2015; Kim et al. 2017; Vincent-Caboud et al. 2019) reporting rye with greater cold tolerance and faster

establishment than triticale in the first months of the winter season. Nevertheless, this trend was not observed in chlorophyll production, as the increase of NDRE displayed similar trends in both rye and triticale. Recently, triticale and barley have been suggested as preferred grasses to be used as CCs compared to rye due to several limitations attributed to the latter (high degree of allelopathy, volunteer cereal rye plants in subsequent phases of the crop rotation, and frequent yield reduction in the subsequent cash crop) (De Bruin et al. 2005; Wells et al. 2016). However, the results of the present study did not show a decrease in maize yield after the rye, and as no differences in SWC after the grasses was observed, there were no symptoms of higher rye pre-emptive competition. On the other hand, rye was a better N scavenger than triticale in 2020, emphasizing its potential for nitrate leaching control. Therefore, the choice between grass species should be made according to the main ecosystem service expected from the CC in each agricultural system (Ramírez-García et al. 2015).

The triticale confirmed in all the 3 years of the present study a soil coverage pattern attributed to catch crops, with a fast increase in autumn followed by a slight decrease in the colder months, before a second rise starts with the increasing temperature in the early spring. Compared to clover in 2021, triticale showed a faster growth until February, as in a previous study (Hirsh et al. 2021), but the same soil coverage (i.e., NDVI, GNDVI, and SAVI) from the end of February till the CC termination. This result was surprising, considering that crimson clover is not even reported as fast as other clover varieties such as Persian clover (Den Hollander et al. 2007). In our study, the early germination before the cold season might have stimulated a faster clover growth in the mild winter of 2021 (Raimondi et al. 2023) as previously reported for warm-season legumes (Butler et al. 2012). This observation confirms the crucial effect of the establishment and termination dates on CC biomass accumulation in the winter season (Duiker 2014).

Looking at the last winter experimental season, mustard CCs showed a larger and faster soil coverage than triticale (with NDVI = 0.75 and GNDVI and SAVI > 0.6 already at the end of October, 1 month and 1 week after the sowing



**Fig. 8** Cumulative dry biomass of cash crops (Mg ha$^{-1}$) (**A**) and cumulative N uptake (kg N ha$^{-1}$) by aboveground biomass of cash crops (**B**) in each CC treatment (Fixed: triticale. Succession: rye in 2020, clover in 2021, mustard in 2022. NoCCs: absence of cover crops) for each experimental season (silage maize in 2020 and 2021; soybean in 2022).
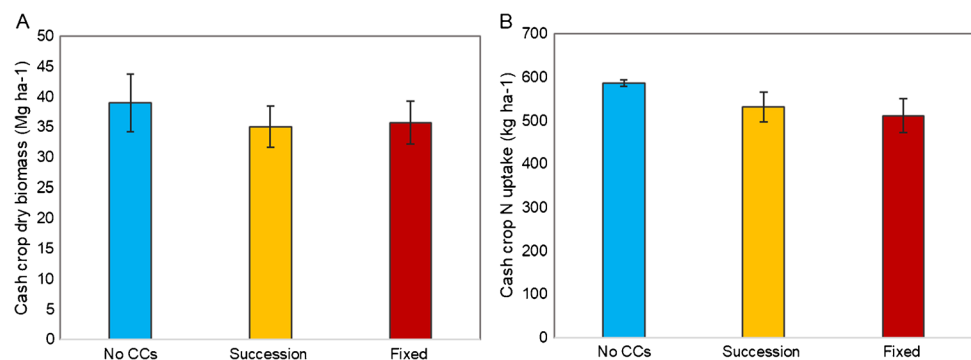
date). However, mustard showed a high susceptibility to the frost event that occurred in the first days of February, confirming previous findings of Gabbrielli et al. (2022). Indeed, after the frost event, mustard was the only winter-killed species, compared to grasses and spontaneous vegetation that showed a growth recovery, as already reported by Koudahe et al. (2022). Early winter-killed mustard plants, laid on the soil, were likely to keep controlling soil erosion (Prabhakara et al. 2015), but at the same time might have resulted in N release from residue decomposition. This early N release might have increased surface soil mineral N concentrations (Hirsh et al. 2021) and, at the same time, the risk of N leaching (Dean and Weil 2009). However, the SWC measurement after the frost event showed a decreasing pattern of SWC up until the end of March (CC termination), which suggested a possible growth activity of the smaller mustard plants that managed to recover after the frost events (being protected by the higher plants). A photographic survey of plants on February 2022 (data not shown) confirmed the presence of small mustard plants growing among the dead residues of the winter-killed plants. These results suggest that N released from the winter-killed mustard residue decomposition might have not been leached but remained potentially available for the following cash crop (Snapp et al. 2005; White et al. 2017).

Despite all the VIs based on the visible and NIR, NDVI identified better the CC growing dynamics compared to NDRE, but NDRE was able to detect the drop of chlorophyll content suffered by the winter-killed plants up to 10 days before the other VIs. This is attributed to the highest sensitivity of the red edge bands to chlorophyll content than the visible bands (Xie et al. 2019). This is also supported by the fact that the NDRE obtained the highest correlation with N uptake in 2020. Different studies demonstrated that the sensitivity of the red edge region to chlorophyll content and N uptake increase with hyperspectral sensors capturing narrow bands of < 5 nm spectral resolution (Berger et al. 2020; Raya-Sereno et al. 2021), as compared to the 15-nm spectral resolution of the Sentinel-2 B6. For this reason, the upcoming satellite missions such as Landsat Next or Copernicus hyperspectral imaging mission for the environment (CHIME) that will provide open-access products with global hyperspectral measurements are expected to provide improvements in the CC dynamics monitoring.

In this study, the VIs analyzed showed good performance in monitoring CCs' growth and parameters. However, due to the empirical basis of the VIs, the reliability of this approach should be tested with different CC species, soils, and climate conditions in order to provide accurate CC management recommendations. This is especially important when using VIs because they are based on the relationship between few spectral bands and therefore ignore information from other wavelengths collected by the sensor, which can lead to a lack of transferability (Camino et al.

2022). For this reason, it is important to test alternative modeling approaches for CC monitoring that rely on the entire spectra, instead of considering only VIs. Modeling approaches such as multiple endmember spectral mixture analyses (MESMA; Roberts et al. 1998) or radiative transfer models like PROSAIL (Jacquemoud et al. 2009) can be an alternative to VIs to enhance CC monitoring with remote sensing techniques and, therefore, should be investigated in future research. The MESMA approach performs fractional cover maps based on pure spectra of the different land cover classes, which can be collected from the same image (Meerdink et al. 2019). MESMA has demonstrated success in detecting agricultural management practices (Shivers et al. 2019) and fractional covers (Dennison et al. 2019) using time series acquisition, but its applicability for CC monitoring remains untested. On the other hand, PROSAIL applied to Sentinel-2 imagery has shown satisfactory results in N uptake monitoring (Bossung et al. 2022). However, the application of PROSAIL specifically for CCs monitoring has only been explored by Wang et al. (2023), who reported promising results in estimating aboveground biomass and N uptake using airborne hyperspectral sensors. Therefore, future research should delve into the potential of these advanced techniques for comprehensive CCs monitoring and management.

The introduction of winter CCs is reported as a valid agronomic practice to improve soil physical properties as well as increase SWC (Malone et al. 2007). In the critical periods of our study (CC termination and before the cash crop sowing in 2021 and 2022), all treatments showed the same SWC in the upper 0–50-cm depth. By the end of winter, after the colder months when the plants' transpiration and the water uptake were at a minimum, the CCs showed a growth resumption with the increasing temperature (both air and soil) and related soil nitrification activity. In this period, there was water consumption by CCs, but it did not impair the SWC available by the time of cash crop sowing, compared to the spontaneous vegetation in the NoCC treatment, confirming previous findings (Alonso-Ayuso et al. 2018a, b). The CCs and the spontaneous species indeed did not make the SWC during summer a limiting factor for maize and soybean final yield production and quality. In 2021 indeed, the maize after both the CC species (triticale and crimson clover) had lower SWC available compared to the NoCC treatment from the end of June until August when maize water demand is usually critical for optimizing yield (NeSmith and Ritchie 1992). In 2022, a similar pattern was observed for the soybean at the beginning of the reproductive stage, which had lower SWC availability after mustard CCs compared to both triticale and NoCC treatments. The low rainfall registered in both the 2020 and 2021 summer seasons might have resulted in the SWC not being sufficient to replenish soil water levels after CC termination; in

addition, the incorporation of the CC residues may not have reduced soil evaporation as much as it is usually reported for residues left on the surface (Dabney 1998; Unger and Vigil 1998). Moreover, CC effect on soil physical property improvement, which can increase infiltration and enhance water storage capacity is usually reported after long-term use of CCs (Steele et al. 2012; García-González et al. 2018; Çerçioğlu et al. 2019), whereas the present study is a 3-year-long experiment. Overall, pre-emptive water competition caused by CCs is the result of multiple factors, and despite the changes in SWC registered during the three seasons, no significant effect on cash crop biomass was observed.

Looking at the CCs' effect on the N dynamics during the whole experimental period, it has been observed that the cumulative final N uptake of the cash crops was the same in the CC and NoCC treatments. Although the model estimated a higher cumulative total quantity of N released from the CC residues in the succession treatment compared to the NoCCs and fixed treatments, it did not affect the final cash crop N uptake. This was likely due to the low amount of N released registered on average in all the treatments, which averaged about 16.3% of the total N uptake of the CCs. This result is related to the total quantity of CC biomass produced in the present study at the termination time (end of March), which was in some cases lower compared to average values registered in other studies conducted in sub-humid regions (Lu et al. 2000; Prieto and Ernst 2012; Ruis et al. 2019). The analysis of the N-release rate estimated by the model in each year of the experimentation allowed to show different patterns in the CC treatments in the 3 years. The simulation showed a net N mineralization from all the CCs and the spontaneous vegetation aboveground biomass residues (in all the experimental years), whereas a net N immobilization from the triticale roots biomass. The N mineralization of the CCs residues showed the same pattern reported in previous studies about CCs incorporated residues (Kuo and Sainju 1998; Lawson et al. 2013; Poffenbarger et al. 2015) with the highest N release rate reached around 2 months after the CC termination, followed by a decreasing rate until the cash crop harvest. A similar pattern was observed for the triticale root residue immobilization, which was highest 2.5 months after the CC termination. Even though it is usually reported that all the triticale biomass residues lead to N immobilization (Rosolem et al. 2018; White et al. 2016), in our study, it was registered only for the root biomass.

The N release pattern, from the CC residues, showed a possible fit with the N requirement pattern of summer cash crops (Raimondi et al. 2021) such as maize (highest N uptake around 30–40 days after planting). It is indeed reported that introducing CCs may result in better synchrony of N mineralization with the N uptake by the subsequent crop (Lara Cabezas et al. 2004). However, the cumulative N released by the CCs in our study was lower than the cash crop N demand. This result

suggests that the pattern of the N release rate from all the CC residues (legumes, brassicas, and grasses), in addition to the amount of N released, should be further investigated in long-term experiments to evaluate their possible contribution to more efficient and sustainable N fertilization.

The N release estimated in the present study also confirmed the potential impact of the environmental conditions on the N mineralization-immobilization processes. Regardless of the CC species, in both the 2020 and 2021 years, increasing trends of the estimated N release rates (after the CCs termination) were estimated in correspondence to both increasing SWC and soil temperature values in rye, clover, and NoCC treatments. These observations confirmed previous results (Torres et al. 2015; Fraser and Hockin 2013; Bontti et al. 2009) showing the crucial impact of SWC and temperature on residue decomposition rates, especially in the early stages after their termination (Soong and Nielsen 2016). Soil moisture and temperature conditions might have also affected the soil micro-fauna, which in turn might have fostered the decomposition rates by increasing detritus surface area through fragmentation and fostering greater microbial colonization (Londoño-R et al. 2013). The CC residue management through incorporation, instead, might have affected less the residue moderation of soil temperature and water content compared to what was observed in the cases of surface application of CC residues (Cook et al. 2010).

The N dynamics, observed over the 3 years, revealed different impacts of CC species and spontaneous vegetation on the N cycle. Interestingly, in the present study, the spontaneous species (starting from the second year of experimentation) showed the same winter soil cover as CCs, and a similar N released quantity than clover (likely due to the high presence of spontaneous clover within the weeds species composition), higher than triticale, during the cash crop season. While the potential of clover as green manure was widely reported (Coombs et al. 2017; Yang et al. 2019), the results of our study demonstrated that further investigations into the potential role of spontaneous vegetation in the N dynamics of conventional agricultural systems might be worthwhile (Li et al. 2020). The results observed for the mustard allowed to confirm previous findings reporting Brassicaceae species as intermediate species between grasses and legumes. It is indeed reported that they can accumulate similar N to grasses in the winter period but decompose faster (thanks to their C:N ratio) supplying substantial plant nutrition similar to legumes (Collins et al. 2007; Finney et al. 2016). Looking at the two grasses species in 2020, rye species showed a higher total N release compared to triticale, despite the same SWC and soil temperature measured in the two treatments. As reported by Thapa et al. (2021, 2022), rye species might show high potential in terms of N release (even

with surface-applied residues), especially when terminated at tillering stage.

In summary, the results of the present study suggested that different CC species might be preferred according to the subsequent cash crops in the agricultural rotation, the environmental conditions of each specific site under analysis, and the main purposes for the CCs introduction. Leguminous species, such as clover, can be considered and evaluated if the main objective is to optimize the N fertilization and reduce fertilization dose. Further study should be conducted to evaluate the CC effect with sub-optimal N fertilization doses. Mustard was revealed as a potential candidate for winter N leaching control and for optimizing cash crop N fertilization. It is highly susceptible to winter climatic conditions though, risking being winter-killed and precociously degraded. Rye and triticale, as grass species, confirmed their validity as catch crops for the winter period. However, long-term experiments with both grasses are needed to better assess their effect on the N nutrition dynamics.

# 5 Conclusions

Optimizing the cover crops' potential benefits on the N dynamics and the soil water content of agricultural systems requires a deep understanding of their growth pattern, N accumulation, and subsequent mineralization.

The use of remote sensing tools, such as satellite images (from which derive VIs) in the present study allowed to reliably monitor the CCs' growing pattern and underlined the site-specific differences among CC species' soil coverage during the winter season. Despite different developments, all the CC species and the spontaneous vegetation in the control treatment used the soil water and N resources for their growth without competing with the subsequent cash crops. The introduction of CCs in the present study did not indeed affect the cash crops yield production and quality.

Nevertheless, the estimation of the CC residue decomposition through a web-based model (CC-NCALC) revealed that CCs in the present study can differently affect the soil N dynamics enhancing N mineralization and N immobilization after incorporation of CC residues of clover and grasses, respectively. The use of the prediction model allowed to estimate the CC N contribution to the subsequent crop. Despite the specific results of the present study (little N contribution estimated from all the CCs likely due to the low CCs biomass production), the application of the model is able to provide information potentially helpful to increase the management efficiency of cash crop N fertilization.

Both the use of prediction model for CC residues' N release and remote sensing tools can be valid instruments to optimize the CC utilization enhancing crop water and the N fertilization management efficiency.

## Declarations

## References

Alonso-Ayuso M, Gabriel JL, Quemada M (2014) The kill date as a management tool for cover cropping success. PLoS ONE 9(10):e109587. https://doi.org/10.1371/journal.pone.0109587

Alonso-Ayuso M, Gabriel JL, García-González I, Del Monte JP, Quemada M (2018a) Weed density and diversity in a long-term cover crop experiment background. Crop Prot 112:103–111. https://doi.org/10.1016/j.cropro.2018.04.012

Alonso-Ayuso M, Quemada M, Vanclooster M, Ruiz-Ramos M, Rodriguez A, Gabriel JL (2018b) Assessing cover crop management under actual and climate change conditions. Sci Total Environ 621:1330–1341. https://doi.org/10.1016/j.scitotenv.2017.10.095

Alvarez R, Steinbach HS, De Paepe JL (2017) Cover crop effects on soils and subsequent crops in the pampas: a meta-analysis. Soil Tillage Res. 170:53–65. https://doi.org/10.1016/j.still.2017.03.005

Barnes EM, Clarke TR, Richards SE, Colaizzi PD, Haberland J, Kostrzewski M, Waller P, Choi C, Riley E, Thompson T, Lascano RJ (2000) Coincident detection of crop water stress, nitrogen status and canopy density using ground based multispectral data. Proc. Fifth Int. Conf. Precis. Agric. 1619

Bates D, Kliegl R, Vasishth S, Baayen H (2015) Parsimonious mixed models. arXiv preprint arXiv:1506.04967

Berger K, Verrelst J, Féret JB, Hank T, Wocher M, Mauser W, Camps-Valls G (2020) Retrieval of aboveground crop nitrogen content with a hybrid machine learning method. Int J Appl Earth Obs Geoinf. 92:102174. https://doi.org/10.1016/j.jag.2020.102174

Bergtold JS, Ramsey S, Maddy L, Williams JR (2019) A review of economic considerations for cover crops as a conservation practice. Renew Agric Food Syst. 34(1):62–76. https://doi.org/10.1017/S1742170517000278

Blanco-Canqui H, Ruis SJ, Proctor CA, Creech CF, Drewnoski ME, Redfearn DD (2020) Harvesting cover crops for biofuel and livestock production: another ecosystem service? J Agron 112(4):2373–2400. https://doi.org/10.1002/agj2.20165

Bontti EE, Decant JP, Munson SM et al (2009) Litter decomposition in grasslands of Central North America (US Great Plains). Glob Chang Biol 15:1356–1363. https://doi.org/10.1111/j.1365-2486.2008.01815.x

Büchi L, Gebhard CA, Liebisch F, Sinaj S, Ramseier H, Charles R (2015) Accumulation of biologically fixed nitrogen by legumes cultivated as cover crops in Switzerland. Plant Soil 393:163–175. https://doi.org/10.1007/s11104-015-2476-7

Butler DM, Rosskopf EN, Kokalis-Burelle N, Albano JP, Muramoto J, Shennan C (2012) Exploring warm-season cover crops as carbon sources for anaerobic soil disinfestation (ASD). Plant Soil 355:149–165. https://doi.org/10.1007/s11104-011-1088-0

Camino C, Araño K, Berni JA, Dierkes H, Trapero-Casas JL, León-Ropero G, Montes-Borrego M, Roman-Écija M, Velasco-Amo MP, Landa BB, Navas-Cortes JA (2022) Detecting Xylella fastidiosa in a machine learning framework using Vcmax and leaf biochemistry quantified with airborne hyperspectral imagery. Remote Sens Environ 282:113281. https://doi.org/10.1016/j.rse.2022.113281

Campi P, Mastrorilli M, Stellacci AM, Modugno F, Palumbo AD (2019) Increasing the effective use of water in green asparagus through deficit irrigation strategies. Agric Water Manag 217:119–130. https://doi.org/10.1016/j.agwat.2019.02.039

Cabrera ML, Kissel DE, Vigil MF (2005) Nitrogen mineralization from organic residues: research opportunities. J Environ Qual 34(1):75–79. https://doi.org/10.2134/jeq2005.0075

Çerçioğlu M, Anderson SH, Udawatta RP, Alagele S (2019) Effect of cover crop management on soil hydraulic properties. Geoderma 343:247–253. https://doi.org/10.1016/j.geoderma.2019.02.027

Chen P, Haboudane D, Tremblay N, Wang J, Vigneault P, Li B (2010) New spectral indicator assessing the efficiency of crop nitrogen treatment in corn and wheat. Remote Sens Environ 114(9):1987–1997. https://doi.org/10.1016/j.rse.2010.04.006

Collins HP, Delgado JA, Alva AK, Follett RF (2007) Use of nitrogen-15 isotopic techniques to estimate nitrogen cycling from a mustard cover crop to potatoes. J Agron 99(1):27–35. https://doi.org/10.2134/agronj2005.0357

Cook JC, Gallagher RS, Kaye JP, Lynch J, Bradley B (2010) Optimizing vetch nitrogen production and corn nitrogen accumulation under no-till management. J Agron 102(5):1491–1499. https://doi.org/10.2134/agronj2010.0165

Coombs C, Lauzon JD, Deen B, Van Eerd LL (2017) Legume cover crop management on nitrogen dynamics and yield in grain corn systems. Field Crops Res 201:75–85. https://doi.org/10.1016/j.fcr.2016.11.001

Cowpertwait PS, Metcalfe AV (2009) Introductory time series with R. Springer Science and Business Media.

Dabney SM (1998) Cover crop impacts on watershed hydrology. JSWC 53(3):207–213

Dabney SM, Delgado JA, Reeves DW (2001) Using winter cover crops to improve soil and water quality. Commun Soil Sci Plant Anal 32(7–8):1221–1250. https://doi.org/10.1081/CSS-100104110

Daughtry CS, Walthall CL, Kim MS, De Colstoun EB, McMurtrey Iii JE (2000) Estimating corn leaf chlorophyll concentration from leaf and canopy reflectance. Remote Sens Environ Remote Sens Environ 74(2):229–239. https://doi.org/10.3184/174751911X556684

Dean JE, Weil RR (2009) Brassica cover crops for nitrogen retention in the Mid-Atlantic Coastal Plain. J Environ Qual 38(2):520–528. https://doi.org/10.2134/jeq2008.0066

De Bruin JL, Porter PM, Jordan NR (2005) Use of a rye cover crop following corn in rotation with soybean in the upper Midwest. J Agron 97(2):587–598. https://doi.org/10.2134/agronj2005.0587

Den Hollander NG, Bastiaans L, Kropff MJ (2007) Clover as a cover crop for weed suppression in an intercropping design: II. Competitive ability of several clover species. Eur J Agron 26(2):104–112. https://doi.org/10.1016/j.eja.2006.08.005

Duiker SW (2014) Establishment and termination dates affect fall-established cover crops. J Agron 106(2):670–678. https://doi.org/10.2134/agronj2013.0246

Fan X, Vrieling A, Muller B, Nelson A (2020) Winter cover crops in Dutch maize fields: variability in quality and its drivers assessed from multi-temporal Sentinel-2 imagery. Int J Appl Earth Obs Geoinf 91:102139. https://doi.org/10.1016/j.jag.2020.102139

Finney DM, White CM, Kaye JP (2016) Biomass production and carbon/nitrogen ratio influence ecosystem services from cover crop mixtures. J Agron 108(1):39–52. https://doi.org/10.2134/agronj15.0182

Fraser LH, Hockin AD (2013) Litter decomposition rates of two grass species along a semi-arid grassland–forest ecocline. J Arid Environ 88:125–129. https://doi.org/10.1016/j.jaridenv.2012.07.009

Gabbrielli M, Perego A, Acutis M, Bechini L (2022) A review of crop frost damage models and their potential application to cover crops. Ital J Agron 17(2). https://doi.org/10.4081/ija.2022.2046

Gabriel JL, Vanclooster M, Quemada M (2014) Integrating water, nitrogen, and salinity in sustainable irrigated systems: cover crops versus fallow. J Irrig Drain 140(9):A4014002

Gabriel JL, Alonso-Ayuso M, García-González I, Hontoria C, Quemada M (2016) Nitrogen use efficiency and fertilizer fate in a long-term experiment with winter cover crops. Eur J Agron 79:14–22. https://doi.org/10.1016/j.eja.2016.04.015

Gabriel JL, Quemada M, Martín-Lammerding D, Vanclooster M (2019) Assessing the cover crop effect on soil hydraulic properties by inverse modelling in a 10-year field trial. Agric Water Manag 222:62–71. https://doi.org/10.5194/hess-2018-372

García-González I, Hontoria C, Gabriel JL, Alonso-Ayuso M, Quemada M (2018) Cover crops to mitigate soil degradation and enhance soil functionality in irrigated land. 2018. Geoderma 322:81–88. https://doi.org/10.1016/j.geoderma.2018.02.024

Gitelson AA, Kaufman YJ, Merzlyak MN (1996) Use of a green channel in remote sensing of global vegetation from EOS-MODIS. Remote Sens Environ 58(3):289–298. https://doi.org/10.1016/S0034-4257(96)00072-7

Godwin DC, Allan Jones C (1991) Nitrogen dynamics in soi-plant systems. Modeling Plant and Soil Systems 31:287–321. https://doi.org/10.2134/agronmonogr31.c13

Hirsh SM, Duiker SW, Graybill J, Nichols K, Weil RR (2021) Scavenging and recycling deep soil nitrogen using cover crops on mid-Atlantic, USA farms. Agric Ecosyst Environ 309:107274. https://doi.org/10.1016/j.agee.2020.107274

Hively WD, Lee S, Sadeghi AM, McCarty GW, Lamb BT, Soroka A, Moglen GE (2020) Estimating the effect of winter cover crops on nitrogen leaching using cost-share enrollment data, satellite remote sensing, and Soil and Water Assessment Tool (SWAT) modeling. JSWC 75(3):362–375. https://doi.org/10.2489/jswc.75.3.362

Huete AR (1988) A soil-adjusted vegetation index (SAVI). Remote Sens Environ 25:295–309. https://doi.org/10.1016/0034-4257(88)90106-X

Jacquemoud S, Verhoef W, Baret F, Bacour C, Zarco-Tejada PJ, Asner GP, François C, Ustin SL (2009) PROSPECT+ SAIL models: a review of use for vegetation characterization. Remote Sens Environ 113:S56–S66. https://doi.org/10.1016/j.rse.2008.01.026

Jennewein JS, Lamb BT, Hively WD, Thieme A, Thapa R, Goldsmith A, Mirsky SB (2022) Integration of satellite-based optical and synthetic aperture radar imagery to estimate winter cover crop performance in cereal grasses. Remote Sens 14(9):2077. https://doi.org/10.3390/rs14092077

Kariyeva J, Van Leeuwen WJ (2011) Environmental drivers of NDVI-based vegetation phenology in Central Asia. Remote Sens 3(2):203–246. https://doi.org/10.3390/rs3020203

Koudahe K, Allen SC, Djaman K (2022) Critical review of the impact of cover crops on soil properties. ISWCR. https://doi.org/10.1016/j.iswcr.2022.03.003

Kuo S, Sainju UM (1998) Nitrogen mineralization and availability of mixed leguminous and non-leguminous cover crop residues in soil. Biol Fertil Soils 26:346–353. https://doi.org/10.1007/s003740050387

Lara Cabezas WAR, Alves BJR, Caballero SSU, Santana DGD (2004) Influência da cultura antecessora e da adubação nitrogenada na produtividade de milho em sistema plantio direto e solo preparado. Ciência Rural 34:1005–1013. https://doi.org/10.1590/S0103-84782004000400006

Lawson A, Fortuna AM, Cogger C, Bary A, Stubbs T (2013) Nitrogen contribution of rye–hairy vetch cover crop mixtures to organically grown sweet corn. Renew Agric Food Syst 28(1):59–69. https://doi.org/10.1017/S1742170512000014

Lee S, Yeo IY, Sadeghi AM, McCarty GW, Hively WD, Lang MW (2016) Impacts of watershed characteristics and crop rotations on winter cover crop nitrate-nitrogen uptake capacity within agricultural watersheds in the Chesapeake Bay region. PLoS ONE 11(6):e0157637. https://doi.org/10.1371/journal.pone.0157637

Lenth R, Singmann H, Love J, Buerkner P, Herve M (2021) Emmeans: estimated marginal means, aka least-squares means. R Package Version 1 (2018)

Li F, Sørensen P, Li X, Olesen JE (2020) Carbon and nitrogen mineralization differ between incorporated shoots and roots of legume versus non-legume based cover crops. Plant Soil 446:243–257. https://doi.org/10.1007/s11104-019-04358-6

Londoño-R LM, Tarkalson D, Thies JE (2013) In-field rates of decomposition and microbial communities colonizing residues vary by depth of residue placement and plant part, but not by crop genotype for residues from two Cry1Ab Bt corn hybrids and their non-transgenic isolines. Soil Biol Biochem 57:349–355. https://doi.org/10.1016/j.soilbio.2012.09.011

Lu YC, Watkins KB, Teasdale JR, Abdulbaki AA (2000) Cover crops in sustainable food production. Food Rev Int 16:121–157. https://doi.org/10.1081/FRI-100100285

Malone RW, Huth N, Carberry PS, Ma L, Kaspar TC, Karlen DL, Heilman P (2007) Evaluating and predicting agricultural management effects under tile drainage using modified APSIM. Geoderma 140(3):310–322. https://doi.org/10.1016/j.geoderma.2007.04.014

Meerdink SK, Roberts DA, Roth KL, King JY, Gader PD, Koltunov A (2019) Classifying California plant species temporally using airborne hyperspectral imagery. Remote Sens Environ 232:111308. https://doi.org/10.1016/j.rse.2019.111308

NeSmith DS, Ritchie JT (1992) Effects of soil water-deficits during tassel emergence on development and yield component of maize (Zea mays). Field Crops Res 28(3):251–256. https://doi.org/10.1016/0378-4290(92)90044-A

Nowak B, Michaud A, Marliac G (2022) Soil-climate factors have a greater influence on the presence of winter cover crops than regulatory constraints in France. ASD 42(2):28. https://doi.org/10.1007/s13593-022-00770-y

Onofri A, Seddaiu G, Piepho HP (2016) Long-term experiments with cropping systems: case studies on data analysis. Eur J Agron 77:223–235. https://doi.org/10.1016/j.eja.2016.02.005

Poeplau C, Don A (2015) Carbon sequestration in agricultural soils via cultivation of cover crops–a meta-analysis. Agric Ecosyst Environ 200:33–41. https://doi.org/10.1016/j.agee.2014.10.024

Prabhakara K, Hively WD, McCarty GW (2015) Evaluating the relationship between biomass, percent groundcover and remote sensing indices across six winter cover crop fields in Maryland, United States. Int J Appl Earth Obs Geoinf 39:88–102. https://doi.org/10.1016/j.jag.2015.03.002

Prieto GS, Ernst O (2012) Effect of legume or grass cover crops and nitrogen application rate on soil properties and corn productivity. Agrociencia 16(3):294-301. https://doi.org/10.31285/AGRO.16.686

QGIS Development Team (2020) QGIS Geographic Information System. Open source Geospatial Foundation

Quemada M, Cabrera ML (1996) Temperature and moisture effects on C and N mineralization from cover crop residues. Plant Soil 189:127–137. https://doi.org/10.1023/A:1004281804058

Quemada M, Cabrera ML, McCracken DV (1997) Nitrogen release from surface-applied cover crop residues: evaluating the CERES-N submodel. J Agron 89(5):723–729. https://doi.org/10.2134/agronj1997.00021962008900050003x

Quemada M, Cabrera ML (2002) Characteristic moisture curves and maximum water content of two crop residues. Plant Soil 238:295–299. https://doi.org/10.1023/A:1014404003851

Raimondi G, Maucieri C, Borin M (2023) Maize yield and N dynamics after cover crops introduction. Eur J Agron 150:126944. https://doi.org/10.1016/j.eja.2023.126944

Raimondi G, Maucieri C, Toffanin A, Renella G, Borin M (2021) Smart fertilizers: what should we mean and where should we go? Ital J Agron 16(2). https://doi.org/10.4081/ija.2021.1794

Ramírez-García J, Carrillo JM, Ruiz M, Alonso-Ayuso M, Quemada M (2015) Multicriteria decision analysis applied to cover crop species and cultivars selection. Field Crops Res 175:106–115. https://doi.org/10.1016/j.fcr.2015.02.008

Raya-Sereno MD, Alonso-Ayuso M, Pancorbo JL, Gabriel JL, Camino C, Zarco-Tejada PJ, Quemada M (2021) Residual effect and N fertilizer rate detection by high-resolution VNIR-SWIR hyperspectral imagery and solar-induced chlorophyll fluorescence in wheat. IEEE Trans Geosci Remote Sens 60:1–17. https://doi.org/10.1109/TGRS.2021.3099624

Roberts DA, Gardner M, Church R, Ustin S, Scheer G, Green RO (1998) Mapping chaparral in the Santa Monica Mountains using multiple endmember spectral mixture models. Remote Sens Environ 65(3):267–279. https://doi.org/10.1016/S0034-4257(98)00037-6

Robertson PG, Gross KL, Hamilton SK, Landis DA, Schmidt TM, Snapp SS, Swinton SM (2014) Farming for ecosystem services:

an ecological approach to production agriculture. Bioscience 64(5):404–415. https://doi.org/10.1093/biosci/biu037

Rouse Jr JW, Haas RH, Deering DW, Schell JA, Harlan JC (1974) Monitoring the vernal advancement and retrogradation (green wave effect) of natural vegetation (No. E75-10354)

Rosolem CA, Castoldi G, Pivetta LA, Ochsner TE (2018) Nitrate leaching in soybean rotations without nitrogen fertilizer. Plant Soil 423:27–40. https://doi.org/10.1007/s11104-017-3494-4

Ruffo ML, Bollero GA (2003) Modeling rye and hairy vetch residue decomposition as a function of degree-days and decomposition-days. J Agron 95(4):900–907. https://doi.org/10.2134/agronj2003.9000

Ruis SJ, Blanco-Canqui H, Creech CF, Koehler-Cole K, Elmore RW, Francis CA (2019) Cover crop biomass production in temperate agroecozones. Agron J 111:1535–1551. https://doi.org/10.2134/agronj2018.08.0535

Shivers SW, Roberts DA, McFadden JP (2019) Using paired thermal and hyperspectral aerial imagery to quantify land surface temperature variability and assess crop stress within California orchards. Remote Sens Environ 222(2019):215–231. https://doi.org/10.1016/j.rse.2018.12.030

Sishodia RP, Ray RL, Singh SK (2020) Applications of remote sensing in precision agriculture: a review. Remote Sens 12(19):1–31. https://doi.org/10.3390/rs12193136

Snapp SS, Swinton SM, Labarta R, Mutch D, Black JR, Leep R, O'neil K, (2005) Evaluating cover crops for benefits, costs and performance within cropping system niches. J Agron 97(1):322–332. https://doi.org/10.2134/agronj2005.0322a

Soong JL, Nielsen UN (2016) The role of microarthropods in emerging models of soil organic matter. Soil Biol Biochem 102:37–39. https://doi.org/10.1016/j.soilbio.2016.06.020

Steele MK, Coale FJ, Hill RL (2012) Winter annual cover crop impacts on no-till soil physical properties and organic matter. SSSAJ 76(6):2164–2173. https://doi.org/10.2136/sssaj2012.0008

Thapa R, Mirsky SB, Tully KL (2018) Cover crops reduce nitrate leaching in agroecosystems: a global meta-analysis. J Environ Qual 47(6):1400–1411. https://doi.org/10.2134/jeq2018.03.0107

Thapa R, Tully KL, Reberg-Horton C, Cabrera M, Davis BW, Fleisher D, Mirsky SB (2022) Cover crop residue decomposition in no-till cropping systems: insights from multi-state on-farm litter bag studies. Agric Ecosyst Environ 326:107823. https://doi.org/10.1016/j.agee.2021.107823

Thieme A, Yadav S, Oddo PC, Fitz JM, McCartney S, King L, Hively WD (2020) Using NASA Earth observations and Google Earth Engine to map winter cover crop conservation performance in the Chesapeake Bay watershed. RSE 248:111943. https://doi.org/10.1016/j.rse.2020.111943

Tolomio M, Borin M (2019) Controlled drainage and crop production in a long-term experiment in North-Eastern Italy. Agric Water Manag 222:21–29. https://doi.org/10.1016/j.agwat.2019.05.040

Torres JLR, Pereira MG, Rodrigues Junior DJ, Loss A (2015) Production, decomposition of residues and yield of maize and soybeans grown on cover crops. Cienc Agron 46:451–459. https://doi.org/10.5935/1806-6690.20150026

Unger PW, Vigil MF (1998) Cover crop effects on soil water relationships. JSWC 53(3):200–207

Vincent-Caboud L, Casagrande M, David C, Ryan MR, Silva EM, Peigne J (2019) Using mulch from cover crops to facilitate organic

no-till soybean and maize production. A Review. ASD 39:1–15. https://doi.org/10.1007/s13593-019-0590-2

Woodruff LK, Kissel DE, Cabrera ML, Habteselassie MY, Hitchcock R, Gaskin J, Rema J (2018) A web-based model of N mineralization from cover crop residue decomposition. SSSAJ 82(4):983–993. https://doi.org/10.2136/sssaj2017.05.0144

Wallander S, Smith D, Bowman M, Claassen R (2021) Cover crop trends, programs, and practices in the United States (No. 1476-2021-709)

Wagger MG, Cabrera ML, Ranells NN (1998) Nitrogen and carbon cycling in relation to cover crop residue quality. JSWC 53(3):214–218

Wang S, Guan K, Zhang C, Jiang C, Zhou Q, Li K, Qin Z, Ainsworth EA, He J, Wu J, Schaefer D (2023) Airborne hyperspectral imaging of cover crops through radiative transfer process-guided machine learning. Remote Sens Environ 285:113386. https://doi.org/10.1016/j.rse.2022.113386

Wittwer RA, van der Heijden MG (2020) Cover crops as a tool to reduce reliance on intensive tillage and nitrogen fertilization in conventional arable cropping systems. Field Crops Res 249:107736. https://doi.org/10.1016/j.fcr.2020.107736

Wells MS, Brinton CM, Reberg-Horton SC (2016) Weed suppression and soybean yield in a no-till cover-crop mulched system as influenced by six rye cultivars. Renew Agric 31(5):429–440. https://doi.org/10.1017/S1742170515000344

White CM, DuPont ST, Hautau M, Hartman D, Finney DM, Bradley B, Kaye JP (2017) Managing the trade off between nitrogen supply and retention with cover crop mixtures. Agric Ecosyst Environ 237:121–133. https://doi.org/10.1016/j.agee.2016.12.016

World Reference Base for Soil Resources (2014) International soil classification systems for naming soils and creating legends for soil maps, World Soil Resources Reports No. 106. FAO, Rome

Xie Q, Dash J, Huete A, Jiang A, Yin G, Ding Y, Peng D, Hall CC, Brown L, Shi Y, Ye H (2019) Retrieval of crop biophysical parameters from Sentinel-2 remote sensing imagery. Int J Appl Earth Obs Geoinf 80:187–195. https://doi.org/10.1016/j.jag.2019.04.019

Yang XM, Drury CF, Reynolds WD, Reeb MD (2019) Legume cover crops provide nitrogen to corn during a three-year transition to organic cropping. J Agron 111(6):3253–3264. https://doi.org/10.2134/agronj2018.10.0652

Yoder BJ, Pettigrew-Crosby RE (1995) Predicting nitrogen and chlorophyll content and concentrations from reflectance spectra (400–2500 nm) at leaf and canopy scales. Remote Sens Environ 53(3):199–211. https://doi.org/10.1016/0034-4257(95)00135-N

## Websites

https://scihub.copernicus.eu/dhus/#/home

INRAE   Springer